https://doi.org/10.5194/acp-2022-676
Preprint. Discussion started: 7 October 2022

Atmospheric Chemistry and Physics Discussions

Technical note: Identification of chemical composition and source of fluorescent components in atmospheric water-soluble brown carbon by excitation-emission matrix with parallel factor analysis: Potential limitation and application

Tao Cao[1,2,3], Meiju Li[1,2,3], Cuncun Xu[1,2,3], Jianzhong Song[1,2,5,*], Xinjun Fan[4], Jun Li[1,2,5], Wanglu Jia[1,2], Ping'an Peng[1,2,3,5]

[1]State Key Laboratory of Organic Geochemistry and Guangdong Provincial Key Laboratory of Environmental Protection and Resources Utilization, Guangzhou Institute of Geochemistry, Chinese Academy of Sciences, Guangzhou 510640, China

[2]CAS Center for Excellence in Deep Earth Science, Guangzhou 510640, China

[3]University of Chinese Academy of Sciences, Beijing 100049, China

[4]College of Resource and Environment, Anhui Science and Technology University, Fengyang 233100, China

[5]Guangdong-Hong Kong-Macao Joint Laboratory for Environmental Pollution and Control, Guangzhou 510640, China

[*]*Correspondence to:* Jianzhong Song, E-mail: songjzh@gig.ac.cn.

https://doi.org/10.5194/acp-2022-676
Preprint. Discussion started: 7 October 2022

Atmospheric Chemistry and Physics Discussions

Abstract

Three-dimensional excitation-emission matrix (EEM) fluorescence spectroscopy is an important method for identification of occurrences, chemical composition, and sources of atmospheric chromophores. However, current knowledge on identification and interpretation of fluorescent components is mainly based on aquatic dissolved organic matter and might not be applicable to atmospheric samples. Therefore, this study comprehensively investigated EEM data of different types of strong light-absorbing organic compounds, water-soluble organic matter (WSOM) in different aerosol samples (combustion source samples and ambient aerosols), soil dust, and purified fulvic and humic acids by an EEM-parallel factor method. The results demonstrated that organic compounds with high aromaticity and strong electron-donating groups generally present strong fluorescence spectra at longer emission wavelength, whereas organic compounds substituted with electron-withdrawing groups have relatively weaker fluorescence intensity. In particular, aromatic compounds containing nitro groups (i.e., nitrophenols), which show strong absorption and are the major component of atmospheric brown carbon, exhibited no significant fluorescence. Although fluorescent component 1 (235, 270/330 nm) in ambient WSOM is generally considered as protein-like groups, our findings suggested that it is mainly composed of aromatic acids, phenolic compounds, and their derivatives, with only traces of amino acids. Principal component analysis and Pearson correlation coefficients between mass absorption efficiency at 365 nm (MAE_{365}) and humification index (HIX), C1, C2, and C3

https://doi.org/10.5194/acp-2022-676
Preprint. Discussion started: 7 October 2022

indicated that the highly aromatic and oxidized fluorescent component 3 may be an important contributor to the light-absorption capacity of ambient WSOM. These findings provide new insights for the analysis of chemical properties and sources of atmospheric fluorophores using the EEM method.

1. Introduction

Brown carbon (BrC) is a class of organic compounds with light absorption in near-ultraviolet and visible wavelength, and is ubiquitous in ambient aerosols, cloud or fog, and rainwater (Fu et al., 2015; Laskin et al., 2015). Owing to its strong light-absorption capacity, BrC can cause up to 45 % solar radiation absorption by atmospheric aerosols, and have potential effects on regional and even global climate (Zhang et al., 2013). In addition, BrC also participates in atmospheric photochemical reactions, affects the physicochemical properties of atmospheric aerosols (Laskin et al., 2015; Tang et al., 2020b), and potentially, can be activated to form reactive oxygen species that cause adverse effects on human health (Bates et al., 2019; Cao et al., 2021).

Excitation-emission matrix (EEM) fluorescence spectroscopy is a highly sensitive and widely used analytical technique for the identification of chemical characteristics and sources of chromophores in dissolved organic matter (DOM) in aquatic environments (Murphy et al., 2010, 2013; Zhang et al., 2014). Recently, EEM has been further extended and frequently applied for the investigation of water-soluble organic matter (WSOM), such as light-absorbing organic compounds

https://doi.org/10.5194/acp-2022-676
Preprint. Discussion started: 7 October 2022

in atmospheric aerosols and fine particles from combustion process (Chen et al., 2020; Fan et al., 2016; Wu et al., 2020). For instance, humic-like substances (HULIS) and protein-like substances (PRLIS) have been identified as important fluorescent components in combustion-derived particles and ambient aerosols (Cao et al., 2021; Matos et al., 2015; Wu et al., 2020). Chen et al. (2016) used EEM coupled with parallel factor analysis (PARAFAC) and high-resolution mass spectrometry to identify chromophores in ambient aerosols, and proposed that fluorescent components with longer excitation (Ex)/emission (Em) wavelengths comprise more highly oxygenated groups (Chen et al., 2016b). In addition, further application of the EEM method has also revealed that the concentration and types of fluorophores obviously vary during atmospheric processes, such as photolytic aging of biomass burning(BB)-derived chromophores (Aftab et al., 2018; Fan et al., 2020; Tang et al., 2020b). Therefore, the EEM method has significant potential for the characterization (types, sources, and evolution) of atmospheric BrC.

However, application of the EEM method for the identification of atmospheric BrC has some limitations. It is well known that the present identification, classification, and interpretation of fluorescent components in atmospheric WSOM are mainly based on the fluorescence peak position of DOM in aquatic environments (Coble, 1996; Wünsch et al., 2019). Nonetheless, the chemical and molecular composition and source of WSOM in atmospheric aerosols significantly vary from those of WSOM in aquatic environments (Graber and Rudich, 2006; Laskin et al., 2015); hence, the current fluorescence criterion derived from aquatic environments

https://doi.org/10.5194/acp-2022-676
Preprint. Discussion started: 7 October 2022

could lead to some inaccurate description of the fluorescent components in atmospheric WSOM. For instance, the EEM region at Ex/Em = 235(270)/330 nm is assigned to PRLIS and/or tryptophan-like substances in aquatic environment (Coble, 1996), but is also associated with non-nitrogen species such as polyphenols in atmospheric WSOM (Chen et al., 2016b). The EEM region at peak M (290–315/370–420 nm) is considered as a typical signal of marine-derived HULIS (Coble, 2007; Zhao et al., 2019), but the source of this peak should be cautiously investigated when interpreting BrC in continental aerosols. In addition, the intensities of fluorescent species are not always linearly correlated with their concentrations, which can be affected by the aromatic ring system, number and types of functional groups, and inner-filter effects (IFEs), thereby leading to a greater uncertainty in intensity measurements (Andrade-Eiroa et al., 2013; Chen et al., 2020; Wang et al., 2020). Atmospheric BrC is composed of complex organic molecules with various properties (Chen et al., 2020), and only a subset of the BrC molecules that contain functional groups are capable of fluorescence emission upon relaxation from an excited state (Andrade-Eiroa et al., 2013). Hence, interpretation of fluorescence data may only correspond to fluorescent chromophores and may not be representative of BrC as a whole (Chen et al., 2020; Wang et al., 2020). All these factors limit further application of the EEM method for the analysis of atmospheric BrC. Therefore, it is essential to investigate the light-absorbing species that can be detected by EEM and obtain important information for identifying the chemical compositions and possible sources of these species.

https://doi.org/10.5194/acp-2022-676
Preprint. Discussion started: 7 October 2022

Accordingly, in the present study, the EEM profiles of a series of BrC model compounds and WSOM isolated from primary combustion samples, soils, and atmospheric aerosols were investigated. The chemical characteristics and sources of the main fluorophores were interpreted according to the fluorescence location and intensity, and the chemical structure of the model compounds and source samples analyzed. Then, atmospheric aerosols in Guangzhou (GZ) and Chuzhou (CZ) cities were collected and fluorescent chromophores within the water-soluble fraction were identified to estimate the application of the EEM-PARAFAC method in characterizing atmospheric BrC. The results obtained help to broaden application of the EEM-PARAFAC method to study atmospheric BrC.

2. Materials and methods

2.1. Materials

For accurate identification of the chemical composition and structures of fluorophores in atmospheric BrC and for assessment of application of the EEM method to examine atmospheric BrC, a total of 136 samples were investigated in this study. The samples comprised: (1) 35 BrC model compounds, including phenolic compounds, aromatic acids, nitroaromatic compounds (NACs), PRLIS, N-heterocyclic compounds, and polycyclic aromatic hydrocarbons (PAHs) and their derivatives (Table S1). These compounds are usually detected in ambient samples and have been considered as the typical BrC model compounds; (2) 13 primary combustion source samples collected from biomass burning, coal combustion(CC),

https://doi.org/10.5194/acp-2022-676
Preprint. Discussion started: 7 October 2022

and vehicle emission (VE); (3) five soil samples obtained from the rural area of Guangdong Province, China, with different vegetation; (4) six purified fulvic and humic acids (FAs and HAs, respectively) kindly provided by Professor Weilin Huang (Rutgers, The State University of New Jersey, NJ, USA); and (5) 34 diurnal fine particulate matter ($PM_{2.5}$) samples collected from 6 to 22 April, 2021 at GZ and CZ, respectively. In addition, 43 annual $PM_{2.5}$ samples were collected from February 2018 to January 2019 at the GZ site and classified as wet and dry season atmospheric $PM_{2.5}$ samples (for detailed information, see Test S1 of supporting information (SI)).

2.2. Standard solution and aqueous extraction of ambient samples

Solutions of model organic compounds were prepared by dissolving a certain amount of dried solid or liquid samples in Milli-Q water or methanol. The ambient aerosol and soil samples were ultrasonically extracted with ultrapure water for three times, and the supernatants were filtered using a 0.22-μm PTFE syringe filter to isolate the WSOM. The specific separation and purification methods have been published in previous studies (Chen et al., 2020; Fu et al., 2015; Wang et al., 2020; Yan and Kim, 2017) and presented in SI (Test S2).

2.3. EEM-PARAFAC analysis

The EEM fluorescence spectra of the aqueous extraction of the samples in 1-cm quartz cuvettes were recorded using a three-dimensional fluorescence spectrophotometer (Aqualog; HORIBA Scientific, USA) at room temperature. The

https://doi.org/10.5194/acp-2022-676
Preprint. Discussion started: 7 October 2022

scanning ranges for Ex and Em was 200–500 and 250–550 nm, respectively. The wavelength increment of the Ex and Em scans was 5 nm, integration time 0.5 s, and Milli-Q water (18.2 Ω) used as blank reference. The absorbance measurements were used to correct the EEM for IFEs as described previously (Fu et al., 2015) if the absorbance was > 0.05 at 250 nm (Murphy et al., 2013; Tang et al., 2020a). Background samples were also analyzed and the background values were subtracted from the values obtained for all the samples. To avoid concentration effects, the fluorescence spectra were normalized by the water Raman area to produce Raman Unit (R.U.) and further by organic carbon concentration of the samples to the normalized fluorescence intensities (R.U./(mg C/L)) (Yang et al., 2022) are shown in Table S2.

The PARAFAC modeling procedure was conducted in MATLAB 2014b (Mathwork.Inc, USA) using the drEEM toolkit (Murphy et al., 2018; Wünsch et al., 2019). The PARAFAC was computed using two to nine component models, with non-negativity constraints and residual analysis, and split-half analysis was employed to validate the number of fluorescent components. Based on the results of the split-half and core consistency analyses, three-component models were chosen for further investigation. The relative contribution of individual chromophores was estimated by calculating the maximum fluorescence intensities (F_{max}: maximum fluorescence intensity of the identified fluorescent components; relative content (%) = $F_{max}/\Sigma F_{max}$) (Chen et al., 2020; Fan et al., 2020).

https://doi.org/10.5194/acp-2022-676
Preprint. Discussion started: 7 October 2022

3. Results and discussion

3.1. Fluorescence properties of BrC model compounds

To identify whether the light-absorbing species possess fluorescence, a series of BrC model compounds were tested by the EEM method, and the fluorescence profiles are shown in Fig. S1. The results revealed that the location and intensity of the fluorescence peaks of different compounds were different, which varied with the distinct functional groups and aromatic conjugate system.

Although phenolic compounds are important light-absorbing species in atmospheric BrC (Smith et al., 2016; Yu et al., 2014, 2016), not all of them exhibit strong fluorescence. As shown in Fig. S1a, a strong fluorescence peak in the EEM spectrum of phenol was observed at Ex/Em = 270/295 nm. When the phenol compounds were substituted with electron-donating groups (e.g., hydroxyl), all of the stronger fluorescence peaks were obviously red-shifted to 310–320 nm (e.g., catechol, hydroquinone, and 2-methoxyphenol). However, phenolic compounds substituted with electron-withdrawing groups (e.g., carboxyl and aldehyde) displayed weaker or even no fluorescence (Fig. S1a). These differences could be owing to the ability of the electron-donating groups to form a larger conjugate system coupled with the benzene ring and decrease the $\pi \rightarrow \pi^*$ transition energy, thus leading to an increase in the Em wavelength (i.e., red shift) and variation in fluorescence intensity. In contrast, the electron-withdrawing group can reduce the conjugate structure formed by the benzene ring and hydroxyl group, reducing the

https://doi.org/10.5194/acp-2022-676
Preprint. Discussion started: 7 October 2022

fluorescence intensity (Andrade-Eiroa et al., 2010; Andrade-Eiroa et al., 2013).

Aromatic acid and its derivatives are also important light-absorbing organic compounds in atmospheric BrC. Owing to the negative effects of carboxyl group, a weak fluorescence peak (275/315 nm) was identified for benzoic acid and no fluorescence was detected for benzene polycarboxylic acids, such as phthalic acid, terephthalic acid, and trimesic acid (Fig. S1b). However, when benzoic acid was substituted with electron-donating groups (e.g., hydroxyl, methoxy), higher intensity fluorescence peaks were observed. Two strong fluorescence peaks at 230/405 and 290/405 nm were identified for 2-hydroxybenzoic acid substituted with only one hydroxyl group. These peaks could have been the result of the ortho structure of the hydroxy and carboxyl groups, which is favorable for the formation of intramolecular hydrogen bond and generates a double-ring conjugate structure, reducing the transition energy and thereby presenting strong UV absorption and fluorescence (Andrade-Eiroa et al., 2013).

The N-containing compounds, especially NACs, have strong light absorption, and have been reported to be the major components of atmospheric BrC, accounting for more than 60 % of the total light absorption intensity at 300–500 nm (Huang et al., 2021; Lin et al., 2016; Lin et al., 2017). However, most of the NACs did not exhibit any fluorescence (Fig. S1c), similar to that reported in a previous study by Chen et al. (2020), which could be owing to the significant reduction in the electron density of benzene ring by the nitro ($-NO_2$) group—strong electron-withdrawing group—thereby weakening the fluorescence.

https://doi.org/10.5194/acp-2022-676
Preprint. Discussion started: 7 October 2022

Tryptophan and tyrosine are the two most studied PRLIS species, and their EEM spectra are generally used as standards for comparison with fluorophores in atmospheric WSOM and aquatic DOM (Coble, 1996, 2007). As shown in Fig. S1d, the Ex/Em peaks at 275/300 and 275/350 nm corresponded to tyrosine and tryptophan, respectively. The maximum Em wavelength of phenylalanine was more inclined to short wavelength (280 nm) and with much weaker fluorescence intensity. Moreover, the fluorescence peaks of PRLIS were obviously overlapped with phenols and aromatic acids (Fig. S1a, b). It must be noted that the concentrations of phenols and aromatic acids were significantly higher than those of tryptophan and tyrosine in the atmospheric samples (Table S2); therefore, the aerosol BrC fluorophores in these regions are more likely to have originated from phenols and aromatic acids rather than PRLIS.

The N-heterocyclic compounds such as pyrrole, pyridine, and imidazole are commonly identified in atmospheric samples (Dou et al., 2015; Jiang et al., 2019; Kosyakov et al., 2020). However, no fluorescence was observed for these three species in the present study, indicating that the absorbed energy may have been consumed by relaxation or vibration (Fig. S1e). Nevertheless, imidazole-2-formaldehyde produced two strong fluorescence peaks at 290/440 and 350/440 nm, formed from the oxidation of imidazole, suggesting that some N-heterocyclic compounds from secondary reaction may exhibit strong fluorescence at higher wavelength in atmospheric BrC (Ackendorf et al., 2017).

PAHs and its derivatives are mainly formed from incomplete combustion

https://doi.org/10.5194/acp-2022-676
Preprint. Discussion started: 7 October 2022

processes, and are important components of BrC (Chen et al., 2020; Lin et al., 2017; Mahamuni et al., 2020). As shown in Fig. S1f, all PAHs exhibited strong fluorescence emission, with its peak location associated with the conjugated aromatic system. Naphthalene presented a fluorescence band located at the maximum Em wavelength of about 325 nm. As expected, with the increasing size of the π-bond system and degree of conjugation, the fluorescence band moved toward the longer wavelength range, and a new Em band was observed at 360–390 nm for 3–4-ring phenanthrene and pyrene, and at 400–500 nm for ≥ 5-ring PAHs (Mahamuni et al., 2020). The fluorescence spectra of high-ring PAHs were more complex because of more types of double bonds. As shown in Fig. S1f, the intensity and location of the fluorescence peaks were also significantly changed when different types of groups were substituted with PAHs. For example, 1-naphthol exhibited stronger EEM peak at a relatively longer wavelength (230, 290/460 nm) owing to its high conjugated structure, when compared with naphthalene. This EEM spectrum was located in the EEM region of FAs, implying that FAs are composed of aromatic units and O-containing groups. In contrast, relatively weaker fluorescence was observed for 9-fluorenone, anthraquinone, and 2-naphthalenecarboxylic acid, and no EEM signals were observed for 2-nitronaphthol (Fig. S1c), which was substituted with a strong electron-withdrawing group ($-NO_2$).

3.2. Fluorescence properties of BrC from different sources

As shown in Fig. S4a and S4b, BB and CC WSOM exhibited similar

https://doi.org/10.5194/acp-2022-676
Preprint. Discussion started: 7 October 2022

fluorescence spectra, with two types of fluorescence peaks at Ex/Em ≈ (230–240)/(340–400) nm (peak A) and Ex/Em ≈ (260–280)/(330–360) nm (peak B), respectively. The two fluorescence peaks were similar to those previously reported for BB WSOM and HULIS (Fan et al., 2020; Tang et al., 2020a; Yang et al., 2022). In general, peak A mainly corresponds to the protein-like UV region, with a minor contribution from fulvic-like substances, whereas peak B could be attributed to tryptophan-like fluorophores. However, based on the results of the present study, these two peaks could be mainly attributed to aromatic species such as aromatic acids, phenolic compounds, and minor quantity of PAHs (e.g., naphthalene) (Fig. 1). The fluorescence spectra of WSOM from two types of vehicles (diesel and gasoline) also presented two fluorophores. A relatively strong fluorescence peak was observed at the low Ex wavelength (Ex/Em ≈ 230/350 nm) and a relatively weaker peak was detected at the high Ex wavelength (Ex/Em ≈ 270/350 nm) (Fig. S4c). These results are consistent with those reported in previous studies on VE (Chen et al., 2020; Tang et al., 2020a; Yang et al., 2022), and similar to the EEM fluorescence spectra of BB and CC WSOM. However, the fluorescence ranges of vehicles WSOM were obviously narrower, suggesting that BB and CC WSOM fluorescent components are more complex.

Soil-derived DOM is also a primary source of atmospheric WSOM. As shown in Fig. S5a, two main fluorescence peaks located at Ex/Em = 230/430 and 320/430 nm, respectively, were detected in the fluorescence spectra of soil DOM, which are similar to those reported in previous studies (Ge et al., 2021; Liu et al., 2009) and

https://doi.org/10.5194/acp-2022-676
Preprint. Discussion started: 7 October 2022

particularly close to the position of FAs (Fig. S5b).

Secondary chemical formation is another important source of atmospheric WSOM. For example, the aqueous-phase reactions of aldehydes with ammonium sulfate (AS) can produce highly fluorescent species (Hawkins et al., 2016). Glyoxal-AS and glyoxal/glycine reaction products fluoresce at 340/450 nm, whereas formaldehyde-AS reaction product fluoresce at 250/430 nm. Secondary organic aerosols (SOAs) produced in the limonene/O_3 system have been reported to strongly fluoresce in the presence of NH_3 (Bones et al., 2010). In addition, aging of primary organic compounds has also been found to change the fluorescence spectra (Lee et al., 2013; Li et al., 2021; Powelson et al., 2014). For instance, aging of syringic acid with OH radicals caused the initial fluorescence band to move toward the long wavelength range, producing a new band at a broad Em band at 400–600 nm. Similarly, the fluorescence peaks red-shifted (e.g., from 260–270/360 nm to 280–290/390–400 nm) during the O_3 aging process (Fan et al., 2020), suggesting the degradation of the initial compound and formation of new secondary organic compounds generally located at longer wavelengths, possibly with a high degree of aromaticity or highly oxidized functional groups (Chen et al., 2016a).

3.3. Identification of chemical species and potential sources of fluorescent components in ambient aerosols

The typical EEM spectra of atmospheric water-soluble light-absorbing compounds are shown in Fig. 2. Three fluorescence peaks were identified in the

https://doi.org/10.5194/acp-2022-676
Preprint. Discussion started: 7 October 2022

aerosol WSOM samples: a stronger fluorescence peak at Ex/Em = 230–250/360–420 nm, and two relative weaker fluorescence peaks at Ex/Em = 270–290/340–370 nm and 300–320/360–420 nm, respectively. Similar fluorescence bands have been previously identified in the EEM fluorescence spectra of WSOM from $PM_{2.5}$ in Xi'an of Northwest China and in Godavari of Nepal (Qin et al., 2018; Wu et al., 2019). Although the fluorescence intensities varied with different sites and seasons, the EEM spectra of WSOM were very similar, making it difficult to directly distinguish the different samples solely based on the characteristics of the EEM profiles. Therefore, a more powerful protocol named the PARAFAC method was employed to identify the individual fluorophores in ambient WSOM.

3.3.1. Identification and quantification of fluorescent components by the PARAFAC method

To better explain the various fluorophores in different atmospheric WSOM samples, the EEM spectra were resolved with the EEM–PARAFAC tool (Andrade-Eiroa et al., 2013; Murphy et al., 2013). As shown in Fig. 3, three fluorescent components (C1, C2, and C3) were identified in the atmospheric samples; C1 occurred at relatively lower Em wavelength, exhibiting two fluorescence peaks at Ex/Em = 235(270)/330 nm, C2 presented fluorescence peaks at around Ex/Em = 235(320)/390 nm, and C3 had a longer Em wavelength than C1 and C2, which was located at Ex/Em = about 250(355)/455 nm. In general, these fluorescent components have been interpreted based on the knowledge of fluorescence

https://doi.org/10.5194/acp-2022-676
Preprint. Discussion started: 7 October 2022

characteristics of aquatic DOM. Accordingly, C1 is considered to belong to the typical PRLIS (Chen et al., 2016a; Chen et al., 2020), C2 is associated with fulvic-like substances or less-oxygenated HULIS (Chen et al., 2016a; Wang et al., 2020), and C3 is usually considered to correspond to terrestrial HULIS that are highly oxygenated organic matter (Table S3) (Chen et al., 2016a; Zhou et al., 2017). However, it must be noted that the sources and transformation process are significantly different for WSOM in aerosols and DOM in aquatic environment; therefore, the fluorescence classifications of DOM might not be applicable to atmospheric WSOM.

In general, the Ex and Em wavelengths of fluorescent components are mainly associated with their chemical characteristics and structures (Table S1 and Fig. 1). In the present study, C1 was similar to tryptophan-like fluorophore associated with PRLIS in rainwater (Zhang et al., 2014; Zhou et al., 2017) and fog water (Bianco et al., 2014; Bianco et al., 2016). However, this fluorophore might also be possibly related to the small molecular aromatic compounds, such as aromatic acids (e.g., 3,5-dihydroxybenzoic acid and 2-naphthalenecarboxylic acid) and PAHs (e.g., naphthalene, phenanthrene, and anthraquinone) (Fig. 1a) (Miyakawa et al., 2015; Wu et al., 2019). In addition, this fluorophore could also contain traces of some phenolic compounds, including catechol, hydroquinone, and 2-methoxyphenol. These organic species might have probably been generated by various types of combustion process and atmospheric oxidation reaction. It must be noted that investigations of the fluorescent components in atmospheric WSOM should not only consider their

https://doi.org/10.5194/acp-2022-676
Preprint. Discussion started: 7 October 2022

position in the fluorescence spectrum, but also their concentration and possibility of trapping. Many previous studies have reported that the concentration of amino acids in the atmospheric aerosols is almost negligible, when compared with that of lower molecular weight aromatic compounds such as aromatic acids and phenolic compounds (Table S2). Therefore, fluorescent components in this Ex/Em region could be attributed to non-nitrogen aromatic species, rather than PRLIS. Moreover, this fluorophore overlapped with that of WSOM from combustion process such as BB, CC, and VE (Fig. 1b), suggesting significant contribution of combustion process.

When compared with C1, C2 exhibited a strong fluorescence peak at longer Ex/Em wavelength of 235(320)/390 nm, implying that this fluorescent component presented relative larger molecular size and higher aromaticity than C1 (Pöhlker et al., 2012). As shown in Fig. 1a, the fluorescence of C2 is similar to that of aromatic compounds (e.g., 2-naphthalenecarboxylic acid, 2-hydroxybenzoic acid, anthraquinone) and high-ring PAHs (e.g., pyrene, anthraquinone, anthracene, chrysene) (Mahamuni et al., 2020), and overlaps with the fluorescence spectra of FAs. In addition, this fluorophore has also been reported to be related to the generation of SOAs from organic precursors emitted from biological/anthropogenic emission and combustion process (Wang et al., 2020). For example, the aqueous-phase reactions of aldehydes with AS has been proposed as an important source of atmospheric BrC, which present similar fluorescence spectral profiles (Hawkins et al., 2016; Lee et al., 2013) (Fig. 1b). Besides, oxidative oligomerization

https://doi.org/10.5194/acp-2022-676
Preprint. Discussion started: 7 October 2022

of phenols and their derivatives can also shift the Ex/Em wavelength of these substances to longer wavelength, falling into similar fluorescence region (Li et al., 2021; Tang et al., 2020a; Vione et al., 2019). As suggested by Chen et al. (2016a), this fluorescent component may be a less-oxygenated fluorescent group contributed by biomass combustion. Therefore, fluorophore C2 might be related to the derivatives of biomass burning and/or biogenic molecules, with relatively lower degree of oxidation (Chen et al., 2016a; Jiang et al., 2022).

C3 presented longer Em wavelength than C1 and C2, with two peaks at around Ex/Em=250/455 nm and 355/455 nm (Fig. 3). This fluorescent component overlaps with the fluorescence of high-ring PAHs and their derivatives, such as fluoranthene, benzo-b-fluoranthene, benzo-a-pyrene, indeno-123cd-pyrene, 1-naphthol, and N-heterocyclic compounds, including imidazole-2-formaldehyde (Chen et al., 2020; Mahamuni et al., 2020). Furthermore, this fluorescent component exhibited similar Ex/Em wavelength to that of FAs and HAs (Fig. S5b), suggesting the possible contribution of soil dust, and thus could be assigned as HULIS (Lin and Guo, 2020). Similar fluorescent substances have also been identified in the study of atmospheric aerosol fluorescent chromophores, such as “HULIS-1” at about 470 nm in Nagoya, Japan (Chen et al., 2016a) and “component 2” at about 480 nm in Godavari, Nepal (Wu et al., 2019). Based on the PARAFAC results with aerosol mass spectrometry data, C3 was considered to be a fluorescent group with high oxygen content and high O/C ratio, close to that of aged organic aerosols (Chen et al., 2016a; Jiang et al., 2022) (Fig. 1b). It must be noted that low molecular weight organic compounds can

https://doi.org/10.5194/acp-2022-676
Preprint. Discussion started: 7 October 2022

further undergo oligomerization to high molecular weight species with long Em wavelength during the aging process (Hawkins et al., 2016; Li et al., 2021; Tang et al., 2020b; Yu et al., 2016). The resulting compounds may present a more complex structure than its precursor, probably owing to the presence of condensed aromatic ring and other π-electron systems with a high level of conjugation; thus, atmospheric aging is assumed to be a potential contributor to C3 (Barsotti et al., 2016; De Laurentiis et al., 2013; Hawkins et al., 2016).

3.3.2. Spatial and seasonal variations of fluorescent components in WSOM

The relative contributions of C1, C2, and C3 components to the total fluorescence intensities ($F_{max}/\sum F_{max}$) were calculated (Fig. 4), and were found to be similar for WSOM from CZ and GZ, exhibiting maximum C2 content and relatively lower C1 and C3 contents. Furthermore, these WSOM samples showed obvious spatial and seasonal variations. First, CZ WSOM presented relatively higher C3 content, whereas GZ WSOM had relatively higher C2 content at the same sampling period. Such differences in the composition of fluorescent components may be ascribed to the variation in the primary emission sources and atmospheric aging process in the two sites. The relatively higher C3 content in CZ could be attributed to the comparatively high contribution of soil dust in the suburban region. In contrast, the relatively higher C2 content in GZ WSOM may be attributed to the comparatively stronger atmospheric chemical reaction associated with bio-volatile organic compounds (bio-VOCs) in the hot and humid region of GZ. This result was

https://doi.org/10.5194/acp-2022-676
Preprint. Discussion started: 7 October 2022

consistent with the relatively higher humification index (HIX) and normalized fluorescence volume (NFV) values (log(NFV)) of CZ WSOM (Fig. S6) (Chen et al., 2020; Yang et al., 2022).

In addition, the resolved Ex and Em spectra for GZ WSOM were also similar in different seasons, implying that the types of fluorophores contributing to WSOM were predominantly the same throughout the year. However, the compositions of fluorescent components varied in different seasons. In the dry season (October–March), WSOM showed relatively higher contents of C3 fluorophores, whereas in the wet season (April–September), slightly higher contents of C2 fluorophores were detected (Fig. 4) (Chen et al., 2020; Wang et al., 2020). These differences might possibly be associated with the variations in the source composition and aging effects of BrC in different seasons. The higher content of C3 in WSOM in the dry season suggested the occurrence of more highly aromatic and highly oxidized compounds. These results could be explained by the fact that more aged organic aerosols and dust were transported from the northern region of China (Jiang et al., 2021). In contrast, the slightly higher C2 content in the wet season may be attributed to the relatively stronger secondary formation of bio-SOAs and photodegradation effects in high-temperature and relative humidity season.

3.4. Correlation with optical and fluorescence properties

It is well known that some organic substances that can generate fluorescence should absorb energy and transit from ground state to excited state and back to

https://doi.org/10.5194/acp-2022-676
Preprint. Discussion started: 7 October 2022

ground state, which could produce corresponding fluorescence. However, it is very difficult to clearly understand the absorption spectra and corresponding fluorescence spectrum of complex WSOM. As indicated in the present study, not all WSOM with strong light absorption exhibit strong fluorescence (e.g., NACs). Hence, to elucidate the association between light-absorbing chromophores and fluorescent components, the relationship between optical properties and fluorophores was analyzed by using principal component analysis and Pearson correlation analysis (Fig. S7). The MAE_{365} showed an obvious positive loading for principal component 1 (PC1) and was grouped with C3 and HIX. Moreover, the MAE_{365} values were positively correlated with C3 and HIX, indicating that light absorption by BrC is more dependent on these fluorophores with long Ex and Em wavelengths and high humification. These results also suggested that the oligomerized fluorescent products with high aromaticity and oxygenated groups may be the dominant factor affecting the light absorption capacity of the fluorescent chromophores. Similar findings have also been reported by Chen et al. (2020) and Tang et al. (2021).

4. Conclusion and future prospects

In this study, the fluorescence properties of BrC model compounds were investigated to determine the chromophoric species that can be evaluated by the EEM method. Accordingly, the aerosol WSOM in two sites (CZ and GZ) were investigated by the EEM-PARAFAC method, and the chemical characteristics and potential sources of fluorescent components were examined. The main conclusions

https://doi.org/10.5194/acp-2022-676
Preprint. Discussion started: 7 October 2022

and future prospects are as follows:

(1) Fluorescent components have predominantly been evaluated based on the knowledge of fluorophores in aquatic DOM, which often leads to misinterpretation. In the present study, the chemical characteristics of fluorophores in different Ex/Em regions were discussed based on the fluorescence properties of BrC model compounds and their amounts in aerosols. In particular, the C1 fluorophore in atmospheric WSOM, which has been frequently assigned to PRLIS because of the similarity in fluorescence spectra, was demonstrated to mainly include aromatic acids, phenolic compounds, and their derivatives, with negligible amount of amino acids.

(2) The fluorescence properties of target compounds are mainly influenced by the aromatic system and characteristics of adjacent functional groups. Organic compounds with high aromaticity and strong electron-donating groups (e.g., hydroxyl, methoxyl) generally exhibited strong fluorescence spectra at longer Em wavelength, whereas organic compounds substituted with electron-withdrawing groups presented relatively weaker fluorescence intensity. In particular, aromatic compounds containing nitro groups (i.e., nitrophenols) showed strong absorption and were the major component of atmospheric BrC; however, they did not exhibit significant fluorescence. Thus, fluorescence method could only measure a subset of chromophores in aerosol BrC and should be used with caution for the investigation of aerosol BrC.

(3) The EEM spectra for aerosol WSOM were very similar; however, the

https://doi.org/10.5194/acp-2022-676
Preprint. Discussion started: 7 October 2022

relative contents of certain fluorescent components significantly varied with the sampling site and season. For example, more fluorescent components associated with dust and secondary oxidation of small molecular compounds from combustion emission were identified in GZ WSOM, whereas more fluorescent components derived from atmospheric chemical reaction of bio-VOCs were observed in CZ WSOM. In addition, GZ WSOM exhibited more highly aromatic and highly oxidized compounds in the dry season.

Although many studies have applied EEM-PARAFAC method to investigate atmospheric WSOM and have obtained useful data, there are still challenges and gaps that must be addressed. First, caution should be taken for credible interpretations of the fluorescent components in atmospheric WSOM because of the differences in chemical characteristics of organic matter derived from different sources. In addition, the same fluorophores may exhibit different Ex/Em ranges and intensities in different environmental conditions (e.g., pH, co-existing metal ions and inorganic salts, etc.). Therefore, more theoretical and experimental studies are necessary to understand the relationship between the fluorescent groups and positions of fluorescence peaks, as well as the influences of sources and chemical formation process of the fluorescent groups on fluorescence peaks.

Data availability

The research data can be accessed in the Harvard Dataverse (https://doi.org/10.7910/DVN/ULCIU9, Song, 2022)

https://doi.org/10.5194/acp-2022-676
Preprint. Discussion started: 7 October 2022

Author contributions. J. Song designed the research. T. Cao and C. Xu, analyzed the model compounds and WSOM samples by UV-Vis and EEM. T. Cao and X. Fan resolved the EEM by PARAFAC tool. M. Li carried out the $PM_{2.5}$ sampling experiments. T. Cao and J. Song wrote the paper. J. Li, W. Jia, and P. Peng commented and revised the paper.

Competing interests. The authors declare that they have no conflict of interest

Acknowledgments. The present work was supported by the National Natural Science Foundation of China (42192514 and 41977188), Guangdong Foundation for Program of Science and Technology Research (2020B1212060053), and Guangdong Foundation for Program of Science and Technology Research (2019B121205006).

References

Ackendorf, J. M., Ippolito, M. G., and Galloway, M. M.: pH Dependence of the Imidazole-2-carboxaldehyde Hydration Equilibrium: Implications for Atmospheric Light Absorbance, Environ. Sci. Tech. Let., 4, 551-555, http://doi.org/10.1021/acs.estlett.7b00486, 2017.

Aftab, B., Shin, H. S., and Hur, J.: Exploring the fate and oxidation behaviors of different organic constituents in landfill leachate upon Fenton oxidation

https://doi.org/10.5194/acp-2022-676
Preprint. Discussion started: 7 October 2022

processes using EEM-PARAFAC and 2D-COS-FTIR, J. Haza. Mat., 354, 33-41, http://doi.org/10.1016/j.jhazmat.2018.04.059, 2018.

Andrade-Eiroa, A., Leroy, V., and Dagaut, P.: Advances in PAHs/nitro-PAHs fractioning, Anal. Meth., 2, 2017, http://doi.org/10.1039/c0ay00484g, 2010.

Andrade-Eiroa, Á., Canle, M., and Cerdá, V.: Environmental Applications of Excitation-Emission Spectrofluorimetry: An In-Depth Review I, Appl. Spec. Rev., 48, 1-49, http://doi.org/10.1080/05704928.2012.692104, 2013.

Barsotti, F., Ghigo, G., and Vione, D.: Computational assessment of the fluorescence emission of phenol oligomers: A possible insight into the fluorescence properties of humic-like substances (HULIS), J. Photo. Photo. A., 315, 87-93, http://doi.org/10.1016/j.jphotochem.2015.09.012, 2016.

Bates, J. T., Fang, T., Verma, V., Zeng, L., Weber, R. J., Tolbert, P. E., Abrams, J. Y., Sarnat, S. E., Klein, M., Mulholland, J. A., and Russell, A. G.: Review of Acellular Assays of Ambient Particulate Matter Oxidative Potential: Methods and Relationships with Composition, Sources, and Health Effects, Environ. Sci. Tech., 53, 4003-4019, http://doi.org/10.1021/acs.est.8b03430, 2019.

Bianco, A., Minella, M., De Laurentiis, E., Maurino, V., Minero, C., and Vione, D.: Photochemical generation of photoactive compounds with fulvic-like and humic-like fluorescence in aqueous solution, Chemosphere, 111, 529-536, http://doi.org/10.1016/j.chemosphere.2014.04.035, 2014.

Bianco, A., Passananti, M., Deguillaume, L., Mailhot, G., and Brigante, M.: Tryptophan and tryptophan-like substances in cloud water: Occurrence and

https://doi.org/10.5194/acp-2022-676
Preprint. Discussion started: 7 October 2022

photochemical fate, Atmos. Environ., 137, 53-61, http://doi.org/10.1016/j.atmosenv.2016.04.034, 2016.

Bones, D. L., Henricksen, D. K., Mang, S. A., Gonsior, M., Bateman, A. P., Nguyen, T. B., Cooper, W. J., and Nizkorodov, S. A.: Appearance of strong absorbers and fluorophores in limonene-O_3 secondary organic aerosol due to $NH4^+$-mediated chemical aging over long time scales, J Geophys Res-Atmos, 115, D05203, http://doi.org/10.1029/2009jd012864, 2010.

Cao, T., Li, M. J., Zou, C. L., Fan, X. J., Song, J. Z., Jia, W. L., Yu, C. L., Yu, Z. Q., and Ping, P. A.: Chemical composition, optical properties, and oxidative potential of water- and methanol-soluble organic compounds emitted from the combustion of biomass materials and coal, Atmos. Chem. Phys., 21, 13187-13205, http://doi.org/10.5194/acp-21-13187-2021, 2021.

Chen, Q., Ikemori, F., and Mochida, M.: Light Absorption and Excitation-Emission Fluorescence of Urban Organic Aerosol Components and Their Relationship to Chemical Structure, Environ. Sci. Tech., 50, 10859-10868, http://doi.org/10.1021/acs.est.6b02541, 2016a.

Chen, Q., Miyazaki, Y., Kawamura, K., Matsumoto, K., Coburn, S., Volkamer, R., Iwamoto, Y., Kagami, S., Deng, Y., Ogawa, S., Ramasamy, S., Kato, S., Ida, A., Kajii, Y., and Mochida, M.: Characterization of Chromophoric Water-Soluble Organic Matter in Urban, Forest, and Marine Aerosols by HR-ToF-AMS Analysis and Excitation-Emission Matrix Spectroscopy, Environ. Sci. Tech., 50, 10351-10360, http://doi.org/10.1021/acs.est.6b01643, 2016b.

https://doi.org/10.5194/acp-2022-676
Preprint. Discussion started: 7 October 2022

Chen, Q., Li, J., Hua, X., Jiang, X., Mu, Z., Wang, M., Wang, J., Shan, M., Yang, X., Fan, X., Song, J., Wang, Y., Guan, D., and Du, L.: Identification of species and sources of atmospheric chromophores by fluorescence excitation-emission matrix with parallel factor analysis, Sci. Total Environ., 718, 137322, http://doi.org/10.1016/j.scitotenv.2020.137322, 2020.

Coble, P. G.: Characterization of marine and terrestrial DOM in seawater using excitation emission matrix spectroscopy, Marin. Chem., 51, 325-346, http://doi.org/10.1016/0304-4203(95)00062-3, 1996.

Coble, P. G.: Marine optical biogeochemistry: The chemistry of ocean color, Chem. Rev., 107, 402-418, http://doi.org/10.1021/cr050350+, 2007.

De Laurentiis, E., Maurino, V., Minero, C., Vione, D., Mailhot, G., and Brigante, M.: Could triplet-sensitised transformation of phenolic compounds represent a source of fulvic-like substances in natural waters?, Chemosphere, 90, 881-884, http://doi.org/10.1016/j.chemosphere.2012.09.031, 2013.

Dou, J., Lin, P., Kuang, B. Y., and Yu, J. Z.: Reactive Oxygen Species Production Mediated by Humic-like Substances in Atmospheric Aerosols: Enhancement Effects by Pyridine, Imidazole, and Their Derivatives, Environ. Sci. Tech., 49, 6457-6465, http://doi.org/10.1021/es5059378, 2015.

Fan, X., Cao, T., Yu, X., Wang, Y., Xiao, X., Li, F., Xie, Y., Ji, W., Song, J., Peng, P., amp, apos, and an: The evolutionary behavior of chromophoric brown carbon during ozone aging of fine particles from biomass burning, Atmos. Chem. Phys., 20, 4593-4605, http://doi.org/10.5194/acp-20-4593-2020, 2020.

https://doi.org/10.5194/acp-2022-676
Preprint. Discussion started: 7 October 2022

Fu, P., Kawamura, K., Chen, J., Qin, M., Ren, L., Sun, Y., Wang, Z., Barrie, L. A., Tachibana, E., Ding, A., and Yamashita, Y.: Fluorescent water-soluble organic aerosols in the High Arctic atmosphere, Sci. Rep., 5, 9845, http://doi.org/10.1038/srep09845, 2015.

Ge, Z., Gao, L., Ma, N., Hu, E., and Li, M.: Variation in the content and fluorescent composition of dissolved organic matter in soil water during rainfall-induced wetting and extract of dried soil, Sci. Total Environ., 791, 148296, http://doi.org/10.1016/j.scitotenv.2021.148296, 2021.

Graber, E. R., and Rudich, Y.: Atmospheric HULIS: How humic-like are they? A comprehensive and critical review, Atmos. Chem. Phys., 6, 729-753, http://doi.org/10.5194/acp-6-729-2006, 2006.

Hawkins, L. N., Lemire, A. N., Galloway, M. M., Corrigan, A. L., Turley, J. J., Espelien, B. M., and De Haan, D. O.: Maillard Chemistry in Clouds and Aqueous Aerosol As a Source of Atmospheric Humic-Like Substances, Environ. Sci. Tech., 50, 7443-7452, http://doi.org/10.1021/acs.est.6b00909, 2016.

Huang, R.-J., Yang, L., Shen, J., Yuan, W., Gong, Y., Ni, H., Duan, J., Yan, J., Huang, H., You, Q., and Li, Y. J.: Chromophoric Fingerprinting of Brown Carbon from Residential Biomass Burning, Environ. Sci. Tech. Let., 9, 102-111, http://doi.org/10.1021/acs.estlett.1c00837, 2021.

Huo, Y. Q., Li, M., Jiang, M. H., and Qi, W. M.: Light absorption properties of HULIS in primary particulate matter produced by crop straw combustion under

https://doi.org/10.5194/acp-2022-676
Preprint. Discussion started: 7 October 2022

different moisture contents and stacking modes, Atmos. Environ., 191, 490-499, http://doi.org/10.1016/j.atmosenv.2018.08.038, 2018.

Jiang, H., Frie, A. L., Lavi, A., Chen, J. Y., Zhang, H., Bahreini, R., and Lin, Y.-H.: Brown Carbon Formation from Nighttime Chemistry of Unsaturated Heterocyclic Volatile Organic Compounds, Environ. Sci. Tech. Let., 6, 184-190, http://doi.org/10.1021/acs.estlett.9b00017, 2019.

Jiang, H., Tang, J., Li, J., Zhao, S., Mo, Y., Tian, C., Zhang, X., Jiang, B., Liao, Y., Song, J., Chen, Y., Zhang, G., 2022. Molecular Signatures of Fluorescence Components in Atmospheric Organic Matters Inferred from Positive and Negative Electrospray Ionization Fourier Transform Ion Cyclotron Resonance Mass Spectrometry. Environ. Sci. Tech. Let., under review.

Jiang, H. X., Li, J., Sun, R., Liu, G. Q., Tian, C. G., Tang, J., Cheng, Z. N., Zhu, S. Y., Zhong, G. C., Ding, X., and Zhang, G.: Determining the Sources and Transport of Brown Carbon Using Radionuclide Tracers and Modeling, J Geophys Res-Atmos, 126, e2021JD034616, http://doi.org/10.1029/2021JD034616, 2021.

Kosyakov, D. S., Ul'yanovskii, N. V., Latkin, T. B., Pokryshkin, S. A., Berzhonskis, V. R., Polyakova, O. V., and Lebedev, A. T.: Peat burning – An important source of pyridines in the earth atmosphere, Environ. Pollut., 266, 115109, http://doi.org/10.1016/j.envpol.2020.115109, 2020.

Laskin, A., Laskin, J., and Nizkorodov, S. A.: Chemistry of atmospheric brown carbon, Chem. Rev., 115, 4335-4382, http://doi.org/10.1021/cr5006167, 2015.

https://doi.org/10.5194/acp-2022-676
Preprint. Discussion started: 7 October 2022

Lee, H. J., Laskin, A., Laskin, J., and Nizkorodov, S. A.: Excitation-emission spectra and fluorescence quantum yields for fresh and aged biogenic secondary organic aerosols, Environ. Sci. Tech., 47, 5763-5770, http://doi.org/10.1021/es400644c, 2013.

Li, F., Tsona, N. T., Li, J., and Du, L.: Aqueous-phase oxidation of syringic acid emitted from biomass burning: Formation of light-absorbing compounds, Sci. Total Environ., 765, 144239, http://doi.org/10.1016/j.scitotenv.2020.144239, 2021.

Lin, H., and Guo, L.: Variations in Colloidal DOM Composition with Molecular Weight within Individual Water Samples as Characterized by Flow Field-Flow Fractionation and EEM-PARAFAC Analysis, Environ. Sci. Tech., 54, 1657-1667, http://doi.org/10.1021/acs.est.9b07123, 2020.

Lin, P., Aiona, P. K., Li, Y., Shiraiwa, M., Laskin, J., Nizkorodov, S. A., and Laskin, A.: Molecular Characterization of Brown Carbon in Biomass Burning Aerosol Particles, Environ. Sci. Tech., 50, 11815-11824, http://doi.org/10.1021/acs.est.6b03024, 2016.

Lin, P., Bluvshtein, N., Rudich, Y., Nizkorodov, S. A., Laskin, J., and Laskin, A.: Molecular Chemistry of Atmospheric Brown Carbon Inferred from a Nationwide Biomass Burning Event, Environ. Sci. Tech., 51, 11561-11570, http://doi.org/10.1021/acs.est.7b02276, 2017.

Liu, L., Song, C., Yan, Z., and Li, F.: Characterizing the release of different composition of dissolved organic matter in soil under acid rain leaching using

https://doi.org/10.5194/acp-2022-676
Preprint. Discussion started: 7 October 2022

three-dimensional excitation-emission matrix spectroscopy, Chemosphere, 77, 15-21, http://doi.org/10.1016/j.chemosphere.2009.06.026, 2009.

Mahamuni, G., Rutherford, J., Davis, J., Molnar, E., Posner, J. D., Seto, E., Korshin, G., and Novosselov, I.: Excitation–Emission Matrix Spectroscopy for Analysis of Chemical Composition of Combustion Generated Particulate Matter, Environ. Sci. Tech., 54, 8198-8209, http://doi.org/10.1021/acs.est.0c01110, 2020.

Matos, J. T. V., Freire, S. M. S. C., Duarte, R. M. B. O., and Duarte, A. C.: Natural organic matter in urban aerosols: Comparison between water and alkaline soluble components using excitation-emission matrix fluorescence spectroscopy and multiway data analysis, Atmos. Environ., 102, 1-10, http://doi.org/10.1016/j.atmosenv.2014.11.042, 2015.

Miyakawa, T., Kanaya, Y., Taketani, F., Tabaru, M., Sugimoto, N., Ozawa, Y., and Takegawa, N.: Ground-based measurement of fluorescent aerosol particles in Tokyo in the spring of 2013: Potential impacts of nonbiological materials on autofluorescence measurements of airborne particles, J Geophys Res-Atmos., 120, 1171-1185, http://doi.org/10.1002/2014jd022189, 2015.

Murphy, K. R., Butler, K. D., Spencer, R. G. M., Stedmon, C. A., Boehme, J. R., and Aiken, G. R.: Measurement of Dissolved Organic Matter Fluorescence in Aquatic Environments: An Interlaboratory Comparison, Environ. Sci. Tech., 44, 9405-9412, http://doi.org/10.1021/es102362t, 2010.

https://doi.org/10.5194/acp-2022-676
Preprint. Discussion started: 7 October 2022

Murphy, K. R., Stedmon, C. A., Graeber, D., and Bro, R.: Fluorescence spectroscopy and multi-way techniques. PARAFAC, Anal. Meth., 5, 6557, http://doi.org/10.1039/c3ay41160e, 2013.

Murphy, K. R., Timko, S. A., Gonsior, M., Powers, L. C., Wünsch, U. J., and Stedmon, C. A.: Photochemistry Illuminates Ubiquitous Organic Matter Fluorescence Spectra, Environ. Sci. Tech., 52, 11243-11250, http://doi.org/10.1021/acs.est.8b02648, 2018.

Pöhlker, C., Huffman, J. A., and Pöschl, U.: Autofluorescence of atmospheric bioaerosols – fluorescent biomolecules and potential interferences, Atmos. Meas. Tech., 5, 37-71, http://doi.org/10.5194/amt-5-37-2012, 2012.

Powelson, M. H., Espelien, B. M., Hawkins, L. N., Galloway, M. M., and De Haan, D. O.: Brown carbon formation by aqueous-phase carbonyl compound reactions with amines and ammonium sulfate, Environ. Sci. Tech., 48, 985-993, http://doi.org/10.1021/es4038325, 2014.

Qin, J., Zhang, L., Zhou, X., Duan, J., Mu, S., Xiao, K., Hu, J., and Tan, J.: Fluorescence fingerprinting properties for exploring water-soluble organic compounds in $PM_{2.5}$ in an industrial city of northwest China, Atmos. Environ., 184, 203-211, http://doi.org/10.1016/j.atmosenv.2018.04.049, 2018.

Smith, J. D., Kinney, H., and Anastasio, C.: Phenolic carbonyls undergo rapid aqueous photodegradation to form low-volatility, light-absorbing products, Atmos. Environ., 126, 36-44, http://doi.org/10.1016/j.atmosenv.2015.11.035, 2016.

https://doi.org/10.5194/acp-2022-676
Preprint. Discussion started: 7 October 2022

Song, J.: Data for CT, Harvard Dataverse [data set], (https://doi.org/10.7910/DVN/ULCIU9, 2022.

Tang, J., Li, J., Su, T., Han, Y., Mo, Y., Jiang, H., Cui, M., Jiang, B., Chen, Y., Tang, J., Song, J., Peng, P. a., and Zhang, G.: M.olecular compositions and optical properties of dissolved brown carbon in biomass burning, coal combustion, and vehicle emission aerosols illuminated by excitation–emission matrix spectroscopy and Fourier transform ion cyclotron resonance mass spectrometry analysis, Atmos. Chem. Phys., 20, 2513-2532, http://doi.org/10.5194/acp-20-2513-2020, 2020a.

Tang, J., Wang, J., Zhong, G., Jiang, H., Mo, Y., Zhang, B., Geng, X., Chen, Y., Tang, J., Tian, C., Bualert, S., Li, J., and Zhang, G.: Measurement report: Long-emission-wavelength chromophores dominate the light absorption of brown carbon in aerosols over Bangkok: impact from biomass burning, Atmos. Chem. Phys., 21, 11337-11352, http://doi.org/10.5194/acp-21-11337-2021, 2021.

Tang, S., Li, F., Tsona, N. T., Lu, C., Wang, X., and Du, L.: Aqueous-Phase Photooxidation of Vanillic Acid: A Potential Source of Humic-Like Substances (HULIS), ACS Ear. Spac. Chem, 4, 862-872, http://doi.org/10.1021/acsearthspacechem.0c00070, 2020b.

Vione, D., Albinet, A., Barsotti, F., Mekic, M., Jiang, B., Minero, C., Brigante, M., and Gligorovski, S.: Formation of substances with humic-like fluorescence properties, upon photoinduced oligomerization of typical phenolic compounds

emitted by biomass burning, Atmos. Environ., 206, 197-207, http://doi.org/10.1016/j.atmosenv.2019.03.005, 2019.

Wünsch, U. J., Bro, R., Stedmon, C. A., Wenig, P., and Murphy, K. R.: Emerging patterns in the global distribution of dissolved organic matter fluorescence, Anal. Meth., 11, 888-893, http://doi.org/10.1039/c8ay02422g, 2019.

Wang, H., Zhang, L., Huo, T., Wang, B., Yang, F., Chen, Y., Tian, M., Qiao, B., and Peng, C.: Application of parallel factor analysis model to decompose excitation-emission matrix fluorescence spectra for characterizing sources of water-soluble brown carbon in $PM_{2.5}$, Atmos. Environ., 223, 117192, http://doi.org/10.1016/j.atmosenv.2019.117192, 2020.

Wu, G., Ram, K., Fu, P., Wang, W., Zhang, Y., Liu, X., Stone, E. A., Pradhan, B. B., Dangol, P. M., Panday, A. K., Wan, X., Bai, Z., Kang, S., Zhang, Q., and Cong, Z.: Water-Soluble Brown Carbon in Atmospheric Aerosols from Godavari (Nepal), a Regional Representative of South Asia, Environ. Sci. Tech., 53, 3471-3479, http://doi.org/10.1021/acs.est.9b00596, 2019.

Wu, G., Fu, P., Ram, K., Song, J., Chen, Q., Kawamura, K., Wan, X., Kang, S., Wang, X., Laskin, A., and Cong, Z.: Fluorescence characteristics of water-soluble organic carbon in atmospheric aerosol, Environ. Pollut., 268, 115906, http://doi.org/10.1016/j.envpol.2020.115906, 2020.

Yan, G., and Kim, G.: Speciation and Sources of Brown Carbon in Precipitation at Seoul, Korea: Insights from Excitation-Emission Matrix Spectroscopy and

Carbon Isotopic Analysis, Environ. Sci. Tech., 51, 11580-11587, http://doi.org/10.1021/acs.est.7b02892, 2017.

Yang, Y., Qin, Y., Qin, J., Zhou, X., Xv, P., Tan, J., and Xiao, K.: Facile Differentiation of Four Sources of Water-Soluble Organic Carbon in Atmospheric Particulates Using Multiple Fluorescence Spectral Fingerprints, Environ. Sci. Tech. Let., 9, 359-365, http://doi.org/10.1021/acs.estlett.2c00128, 2022.

Yu, L., Smith, J., Laskin, A., Anastasio, C., Laskin, J., and Zhang, Q.: Chemical characterization of SOA formed from aqueous-phase reactions of phenols with the triplet excited state of carbonyl and hydroxyl radical, Atmos. Chem. Phys., 14, 13801-13816, http://doi.org/10.5194/acp-14-13801-2014, 2014.

Yu, L., Smith, J., Laskin, A., George, K. M., Anastasio, C., Laskin, J., Dillner, A. M., and Zhang, Q.: Molecular transformations of phenolic SOA during photochemical aging in the aqueous phase: competition among oligomerization, functionalization, and fragmentation, Atmos. Chem. Phys., 16, 4511-4527, http://doi.org/10.5194/acp-16-4511-2016, 2016.

Zhang, X. L., Lin, Y. H., Surratt, J. D., and Weber, R. J.: Sources, Composition and Absorption Angstrom Exponent of Light-absorbing Organic Components in Aerosol Extracts from the Los Angeles Basin, Environ. Sci. Tech., 47, 3685-3693, http://doi.org/10.1021/es305047b, 2013.

Zhang, Y. L., Gao, G., Shi, K., Niu, C., Zhou, Y. Q., Qin, B. Q., and Liu, X. H.: Absorption and fluorescence characteristics of rainwater CDOM and

https://doi.org/10.5194/acp-2022-676
Preprint. Discussion started: 7 October 2022

contribution to Lake Taihu, China, Atmos. Environ., 98, 483-491, http://doi.org/10.1016/j.atmosenv.2014.09.038, 2014.

Zhao, W. Y., Fu, P. Q., Yue, S. Y., Li, L. J., Xie, Q. R., Zhu, C., Wei, L. F., Ren, H., Li, P., Li, W. J., Sun, Y. L., Wang, Z. F., Kawamura, K., and Chen, J. M.: Excitation-emission matrix fluorescence, molecular characterization and compound-specific stable carbon isotopic composition of dissolved organic matter in cloud water over Mt. Tai, Atmos. Environ., 213, 608-619, http://doi.org/10.1016/j.atmosenv.2019.06.034, 2019.

Zheng, G., He, K., Duan, F., Cheng, Y., and Ma, Y.: Measurement of humic-like substances in aerosols: a review, Environ. Pollut., 181, 301-314, http://doi.org/10.1016/j.envpol.2013.05.055, 2013.

Zhou, Y., Yao, X., Zhang, Y., Shi, K., Zhang, Y., Jeppesen, E., Gao, G., Zhu, G., and Qin, B.: Potential rainfall-intensity and pH-driven shifts in the apparent fluorescent composition of dissolved organic matter in rainwater, Environ. Pollut., 224, 638-648, http://doi.org/10.1016/j.envpol.2017.02.048, 2017.

https://doi.org/10.5194/acp-2022-676
Preprint. Discussion started: 7 October 2022

Atmospheric Chemistry and Physics Discussions

(a)

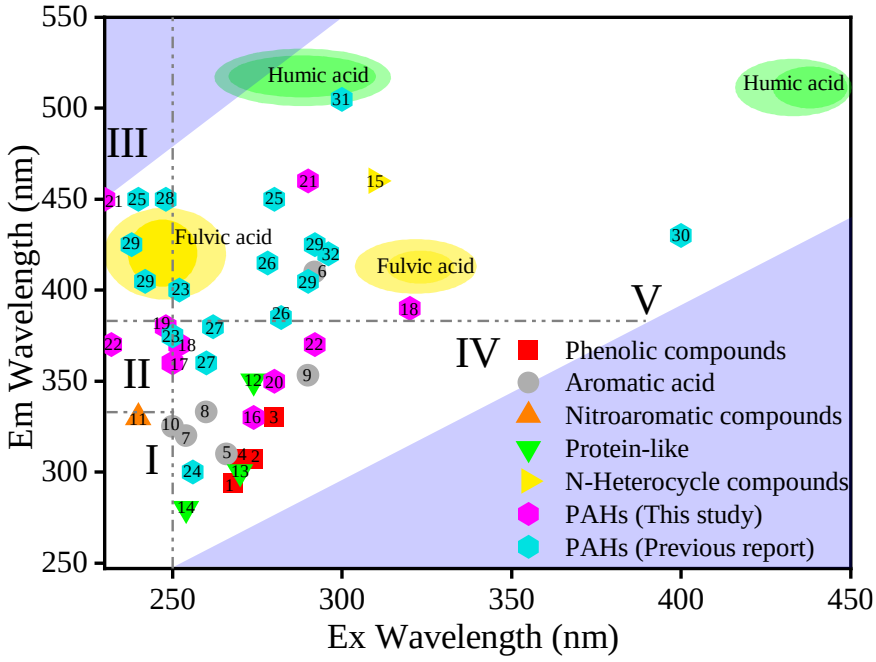

1: Phenol	2: Catechol	3: Hydroquinone
4: 2-Methoxyphenol	5: Benzoic acid	6: 2-Hydroxybenzoic acid
7: 4-Hydroxybenzoic acid	8: 4-Hydroxy-3, 5-dimethoxybenzoic acid	9: 3, 5-Dihydroxybenzoic acid
10: Vanillic acid	11: 4-Nitrocatechol	12: DL-Tryptophan
13: DL-Tryosine	14: Phenylalanine	15: midazole-2-formaldehyde
16: Naphthalene	17: Phenanthrene	18: Pyrene
19: Anthraquinone	20: 9-Fluorenone	21: 1-Naphthol
22:2-Napphthalenecarboxylic acid	23: Anthracene	24: Fluorene
25: Fluoranthene	26: Benzo-a-Anthracene	27: Chrysene
28: Benzo-b-Fluoranthene	29: Benzo-k-Fluoranthene	30: Perylene
31: Indeno-123cd-Pyrene	32: Benzo-ghi-Perylene	

https://doi.org/10.5194/acp-2022-676
Preprint. Discussion started: 7 October 2022

Atmospheric Chemistry and Physics Discussions

(b)

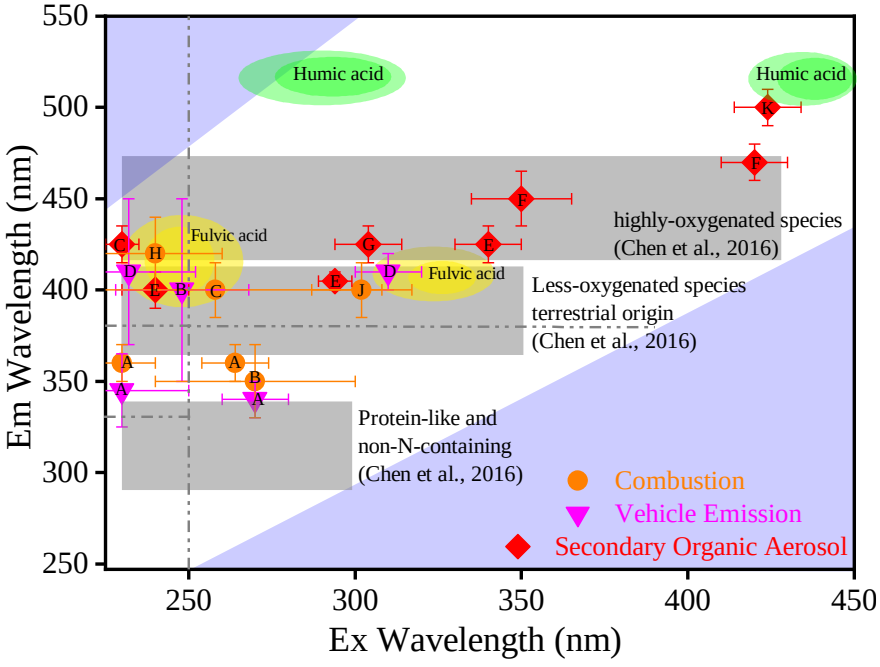

A: This study	B: Yang et al., 2022
C: Chen et al., 2020	D: Tang et al., 2020b
E: Hawkins et al., 2016	F: Bones et al., 2010
G: Lee et al., 2013	H: Mahamuni et al., 2020
J: Yan and Kim 2017	K: Powelson et al., 2014

Figure 1. Comparison of chemical characteristics of molecules assigned to each fluorescence component of BrC model compounds (a) and source WSOM (b).

https://doi.org/10.5194/acp-2022-676
Preprint. Discussion started: 7 October 2022

Atmospheric Chemistry and Physics Discussions

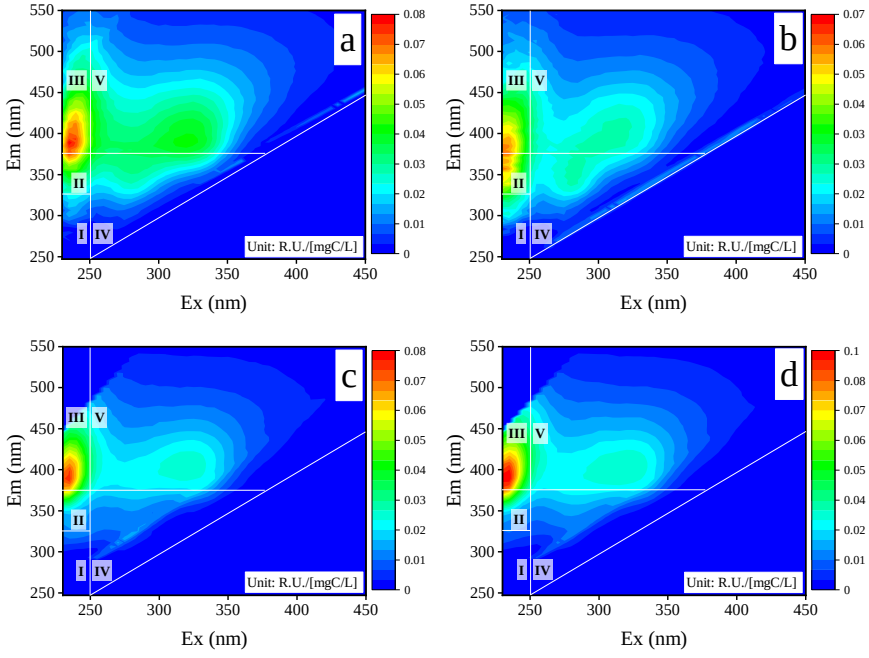

Figure 2. The 3D-EEM spectra of WSOM in atmospheric $PM_{2.5}$ samples (a: Chuzhou (CZ); b: Guangzhou (GZ); c: GZ wet season; d: GZ dry season)

https://doi.org/10.5194/acp-2022-676
Preprint. Discussion started: 7 October 2022

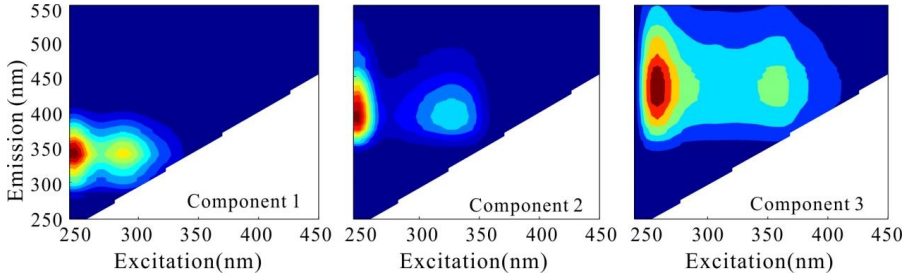

Figure 3. The EEM components derived from the PARAFAC model of WSOC in atmospheric $PM_{2.5}$ samples collected at Chuzhou (CZ) and Guangzhou (GZ) sites.

https://doi.org/10.5194/acp-2022-676
Preprint. Discussion started: 7 October 2022

Atmospheric Chemistry and Physics Discussions

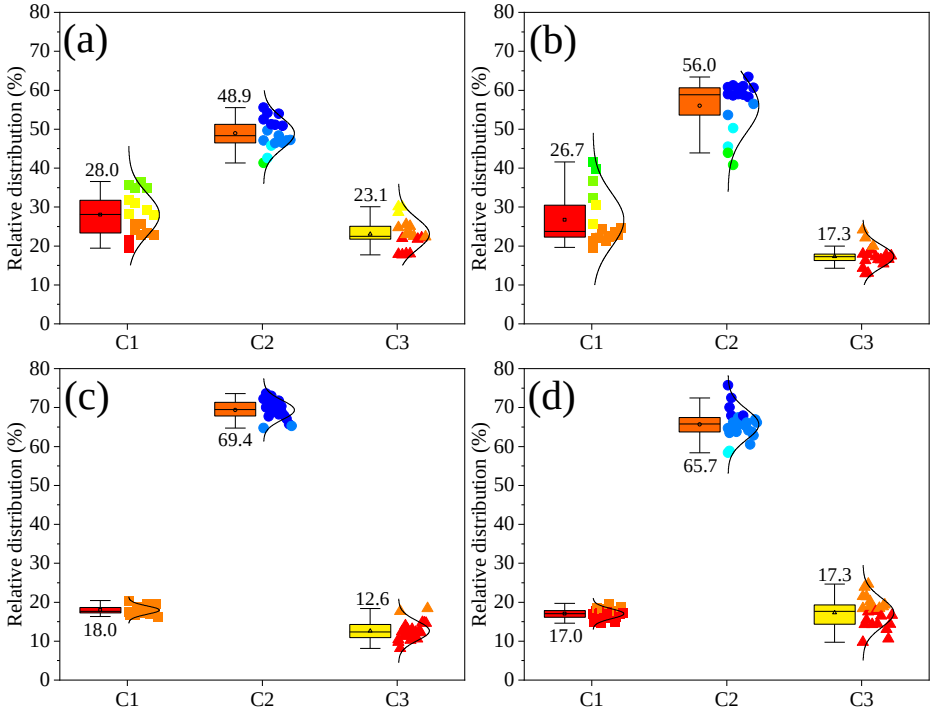

Figure 4. Relative contribution of individual fluorophores of atmospheric WSOM. (a: Chuzhou (CZ); b: Guangzhou (GZ); c: wet season of GZ; d: dry season of GZ)